Supporting information

Double charge carrier mechanism through 2D/2D interface assisted ultrafast water reduction and antibiotic degradation over architecting S, P co-doped g-C_3N_4/ZnCr LDH photocatalyst

Dipti Prava Sahoo, Kundan Kumar Das, Sulagna Patnaik, Kulamani Parida*

Centre for Nano Science and Nano Technology, Siksha O Anusandhan (Deemed to be) University, Bhubaneswar-751030

*Corresponding Author: K.M. Parida

E-mail: kulamaniparida@soauniversity.ac.in & paridakulamani@yahoo.com Tel. No: +91-674-2351777; Fax: +91-674-2350642

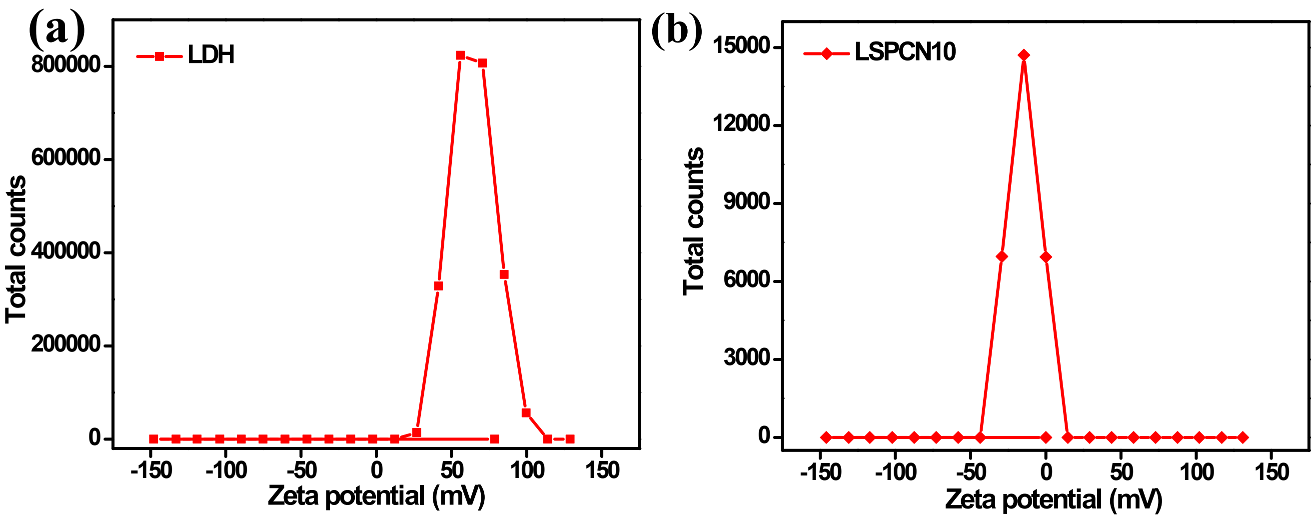

Fig. S1 Zeta potentials of (a) LDH and (b) LSPCN10 samples.

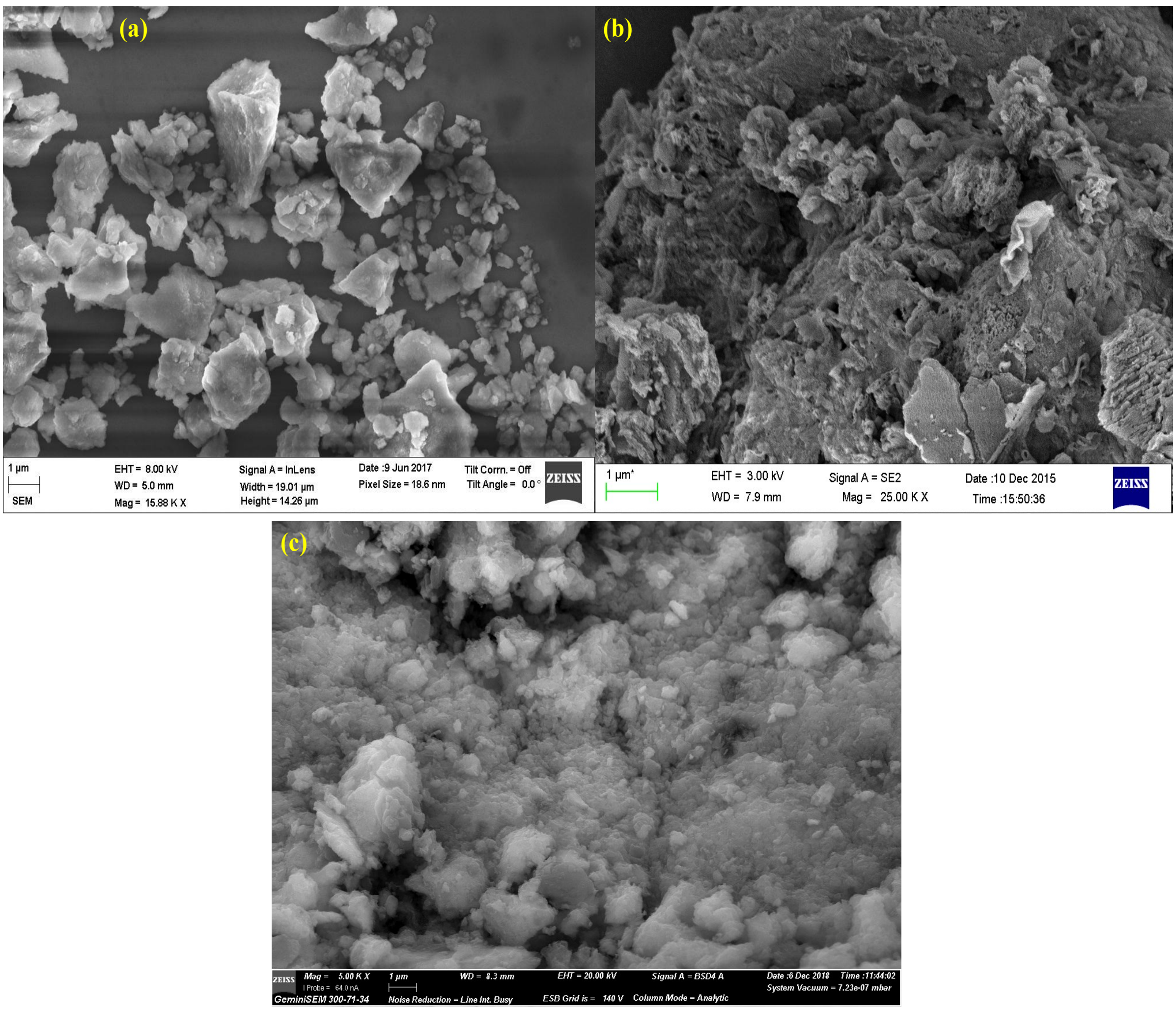

Fig. S2 SEM images of (a) LDH, (b) SPCN (c) LSPCN10 material.

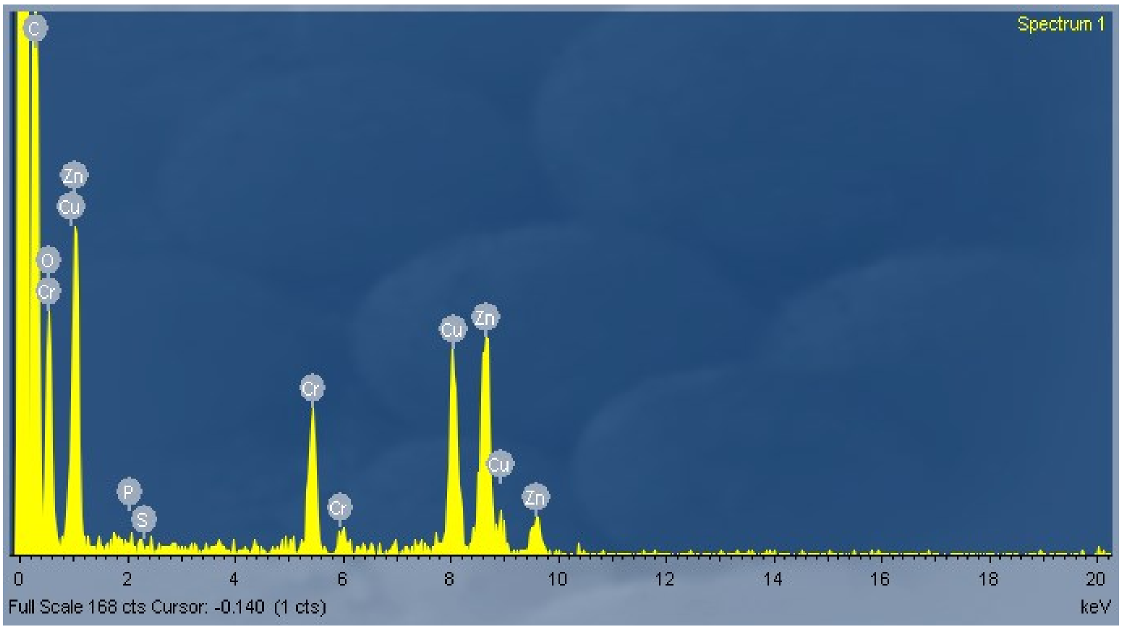

Fig. S3 EDX elemental analysis of LSPCN10 material.

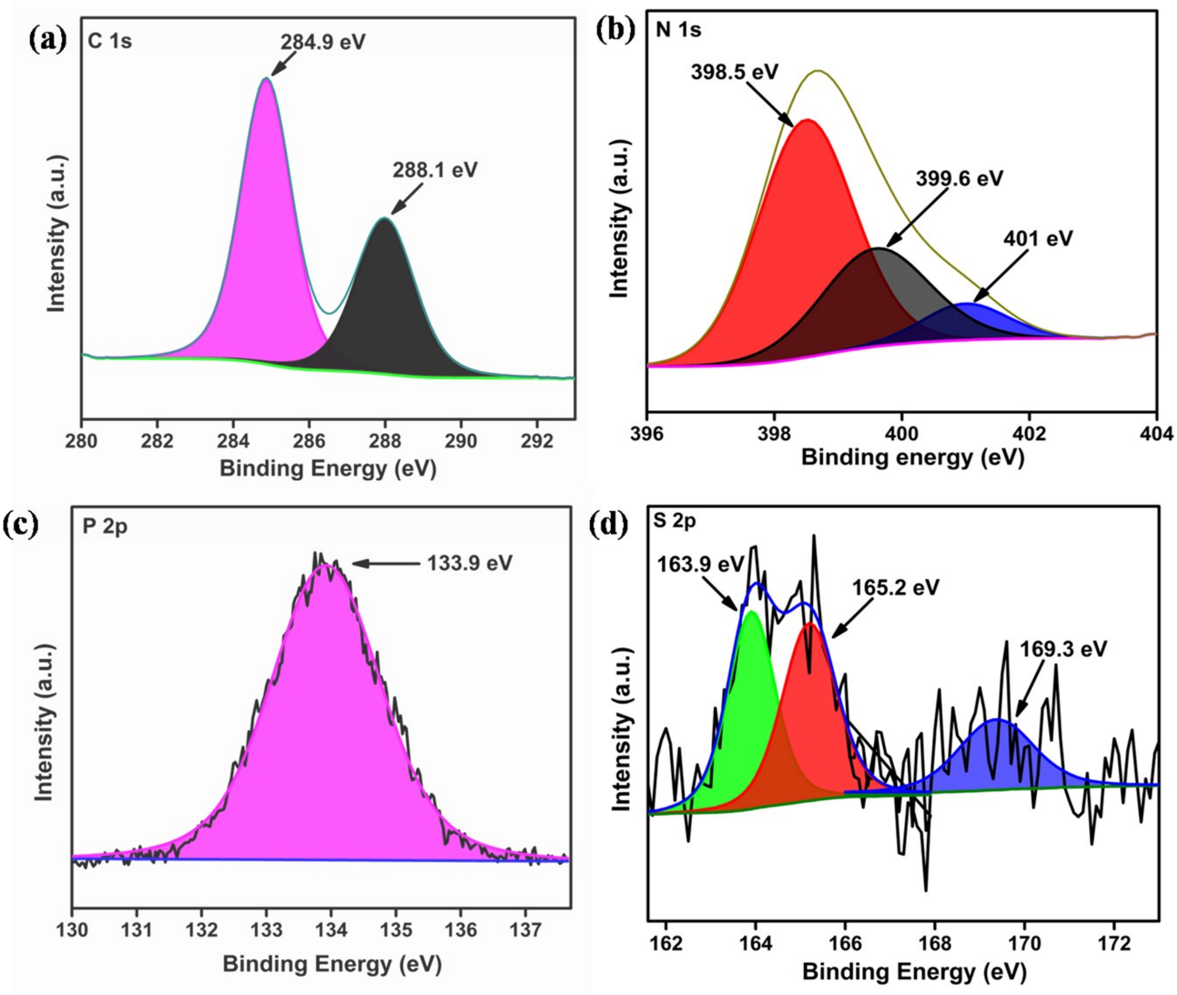

Fig. S4 High resolution deconvoluted XPS spectra of SPCN: (a) C 1s, (b) N 1s, (c) P 2p and (d) S 2p.

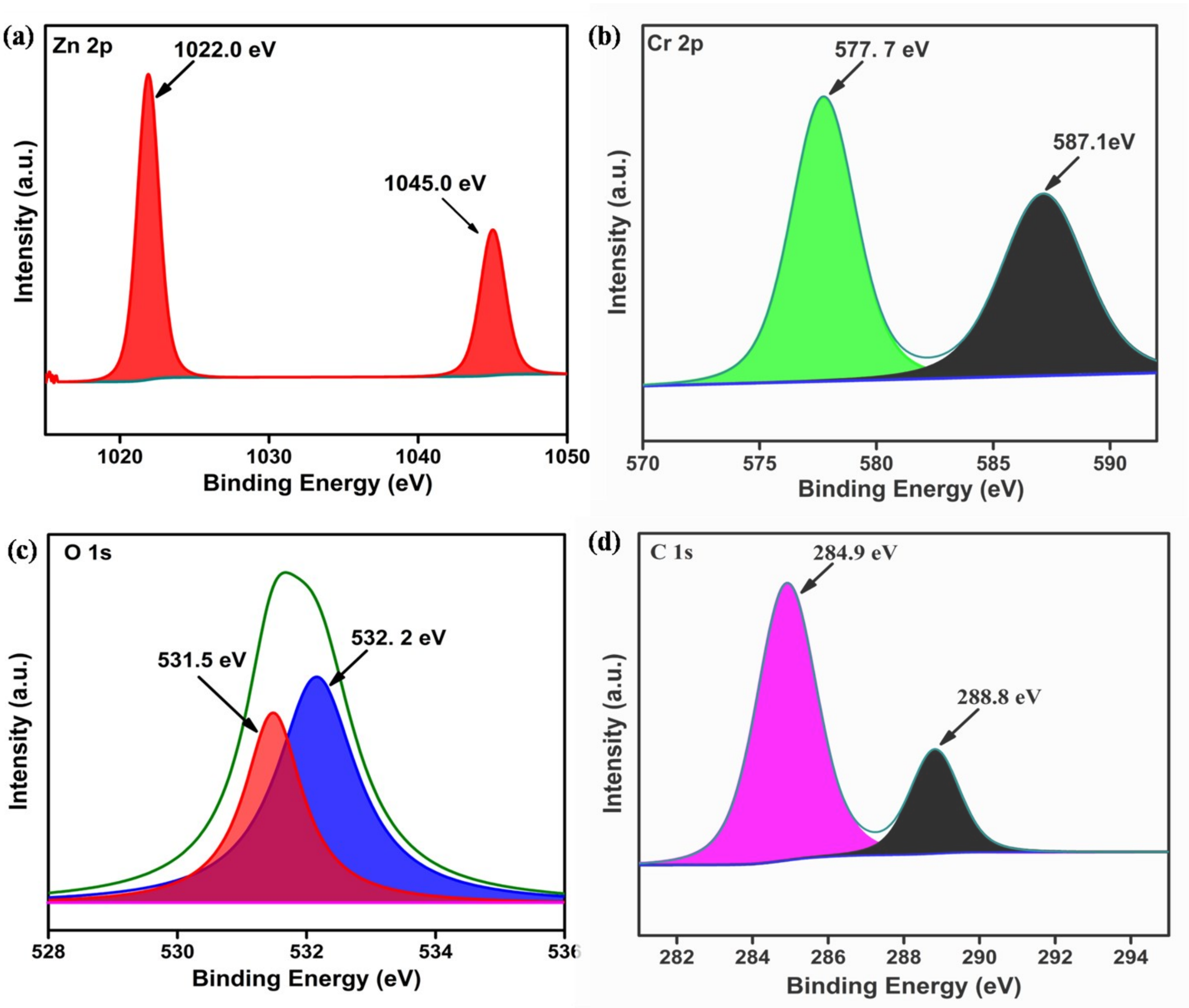

Fig. S5 High resolution deconvoluted XPS spectra of LDH: (a) Zn 2p, (b) Cr 2p, (c) O 2p and (d) C 1s.

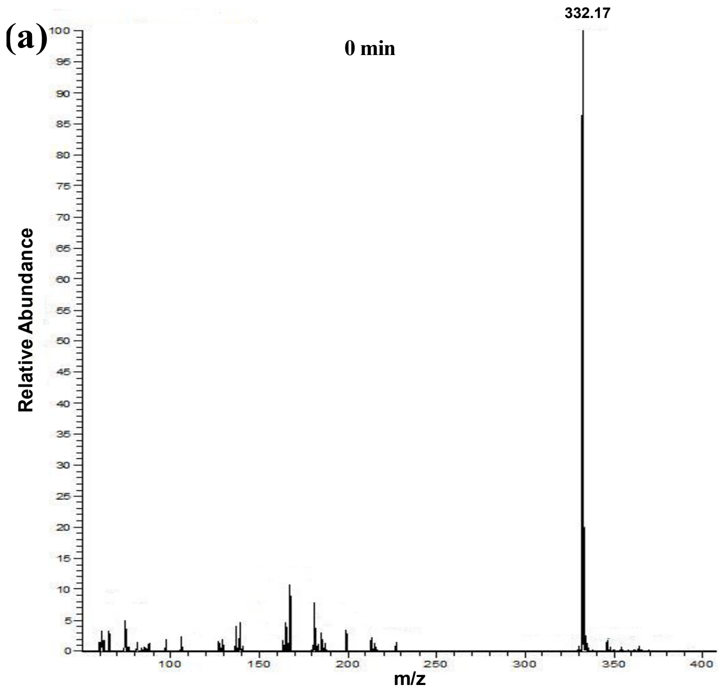
(a)
0 min
332.17
Relative Abundance
m/z

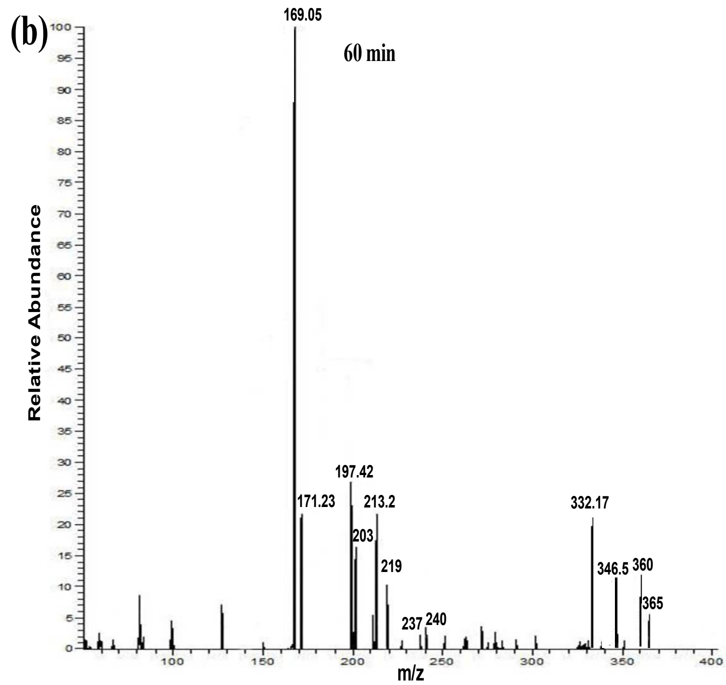
(b)
60 min
169.05
197.42
171.23
213.2
203
219
237
240
332.17
346.5
360
365
Relative Abundance
m/z

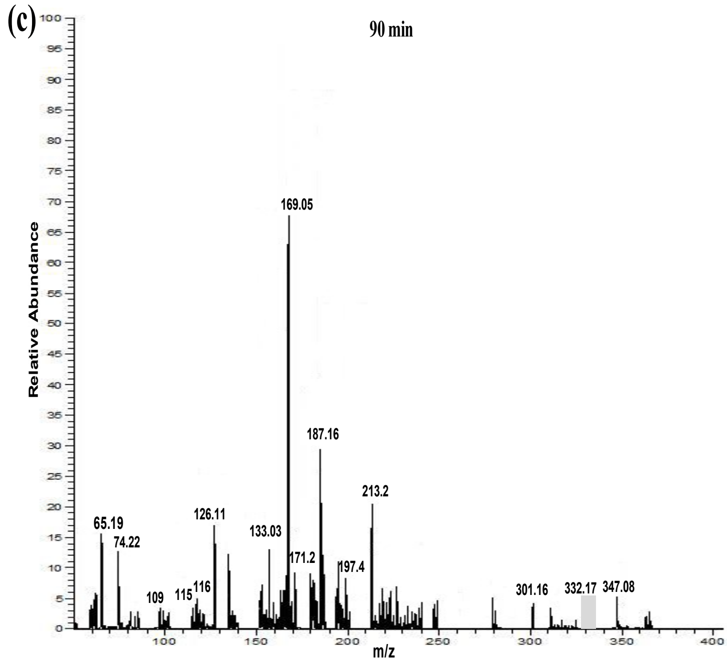

Fig. S6 LC-MS of CPX solution during degradation process over LSPCN10 heterostructure: (a) 0 min, (b) 60 min and (c) 90 min.

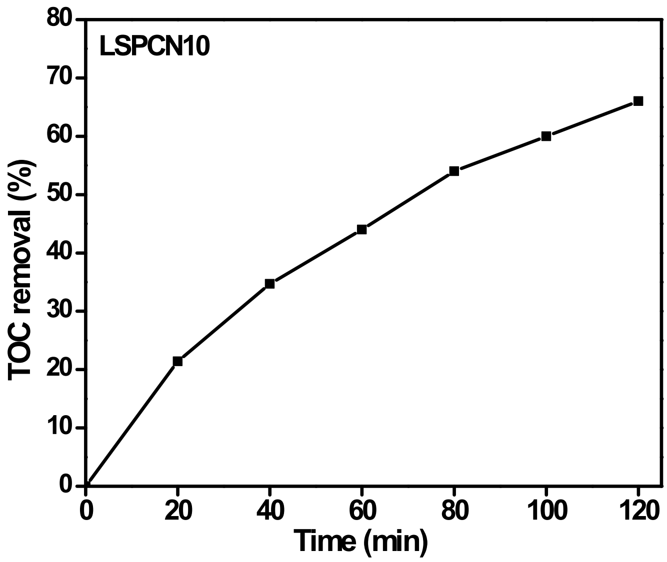

Fig. S7 TOC removal of photocatalytic CPX degradation over LSPCN10.

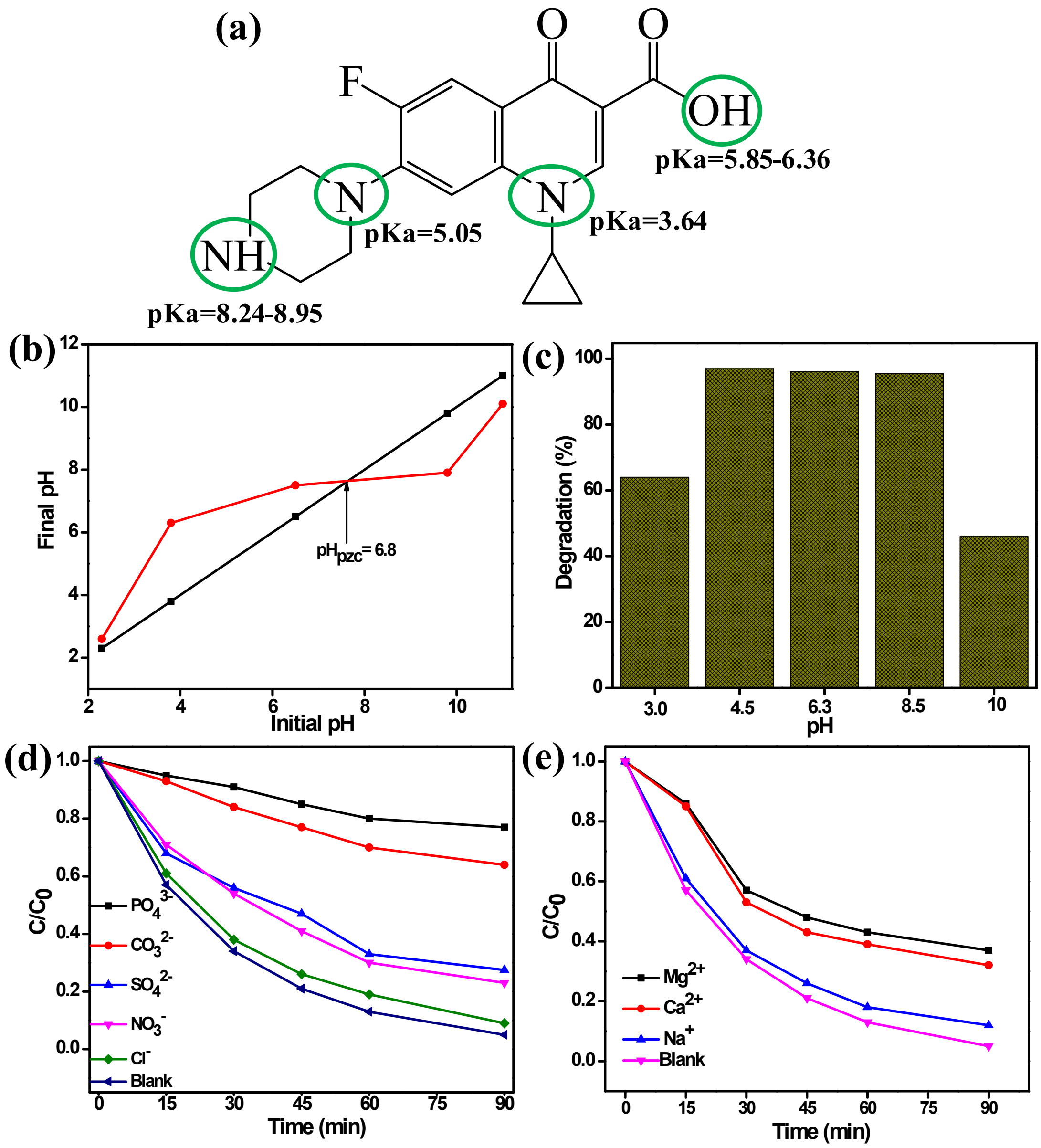

Fig. S8 (a) Molecular structure of CPX ($C_{17}H_{18}FN_3O_3$), (b) PZC plot of LSPCN10 heterostructure, photocatalytic degradation of CPX under (c) different pH, various (d) anions and (e) cations.

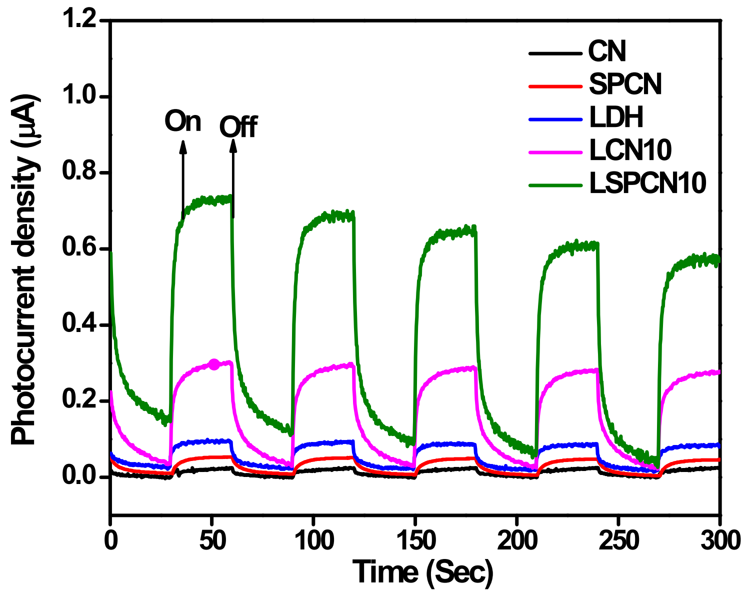

Fig. S9 Transient Photocurrent response analysis of CN, SPCN, LDH, LCN10 and LSPCN10 under discontinuous visible light irradiation.

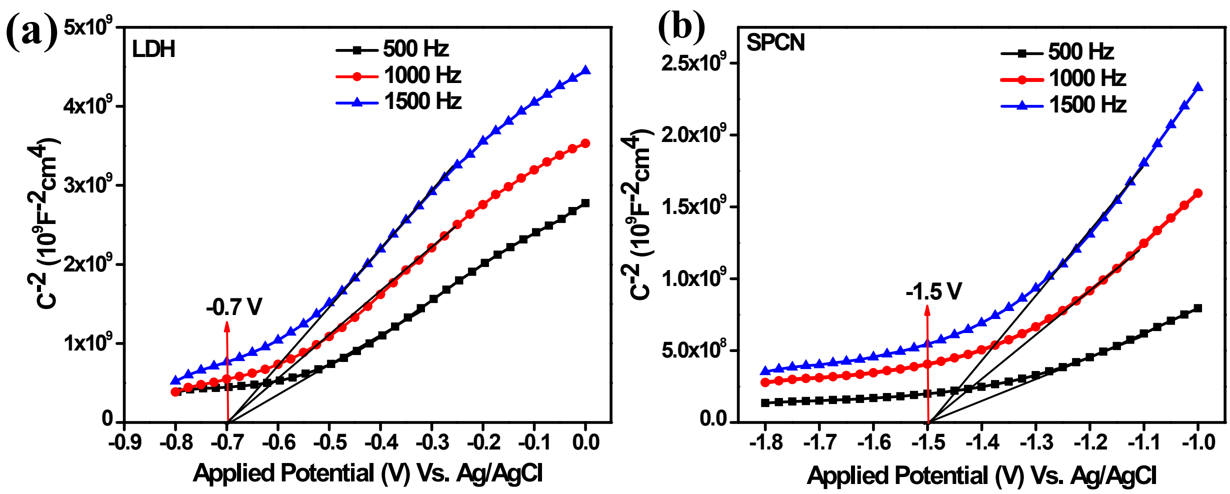

Fig. S10 Mott-Schottky plot of (a) LDH and (b) SPCN at different frequencies.

Table S1 A comparison study for photocatalytic ciprofloxacin degradation over present heterostructure with the reported g-C_3N_4 and LDH based system.

Photocatalysts	Reaction condition (visible light source, CPX concentration, catalyst dosage and time period)	CPX degradation efficiency	Ref
NiAl LDH/Fe_3O_4-RGO	500 W Xe, (λ≥420), 10 ppm CPX solution, (40 ml) 10 mg, 150 min	91%	1

NiAlFe LDH/RGO	500W Xe, (λ≥420), 10 ppm CPX solution (40 mL), 10 mg, 120 min	92%	2
SO_4^{2-}-g-C_3N_4/Ag_3PO_4	400W Xe, (λ≥420), 20 ppm CPX solution (50mL), 20 mg, 50 min	>90%	3
Ag@P-g-C_3N_4/$BiVO_4$	300W Xe, (λ≥420), 10 ppm CPX solution (50mL), 25mg, 120 min	93 %	4
C-dot@ nitrogen deficient g-C_3N_4	300W Xe, (λ≥420), 10 ppm CPX solution (20mL), 20mg, 360 min	3.5 times more than g-C_3N_4	5
g-C_3N_4-TiO_2	300W Xe, (λ≥420), 10 ppm CPX solution (80mL), 30mg, 180 min	85%	6
NiAg/ g-C_3N_4/$Cd_2Sb_2O_{6.8}$	Sun light, 20 ppm CPX solution (50mL), 50mg, 70 min	82%	7
LSPCN10 (Present research)	250 wt medium pressure Hg (λ≥420 nm), 20 ppm CPX solution (20 mL), 20 mg, 90 min	95%	

Table S2 A comparison study for photocatalytic H_2 evolution over present heterostructure with the reported g-C_3N_4 and LDH based system.

Photocatalyst	Visible light source and sacrificial agents	H_2 evolution ($\mu molg^{-1}h^{-1}$)	Ref
CdSe/ZnCr LDH	450 W Xe (λ≥420), Na_2SO_4/Na_2S /Pt	1560	8
CdZnS/ZnCr LDH	300 W Xe, (λ≥420), CH_3OH	18320	9
g-C_3N_4/NiFe LDH	125 W Hg (λ≥420), CH_3OH	24800	10

$RGO/La_2Ti_2O_7$/NiFe LDH	100 mW AM 1.5, (λ≥420), TEOA	532	11
ZnCr LDH/g-C_3N_4	300 W Xe (λ≥420), TEOA	156	12
1 wt% Pt/ NiS/P-S g-C_3N_4	125 W Hg (λ≥420), TEOA,	1805	13
3 wt% Pt/g-C_3N_4/Ti_3C_2	250 W Hg, (λ≥420), TEOA	72.3	14
CoAl LDH/ g-C_3N_4	300 W Xe, (λ≥420), TEOA	680	15
$Co(OH)_2$/ZnCr LDH	125 W Hg, (λ≥420), CH_3OH	27875	16
WO_{3-X}/Ag/ZnCr LDH	150 W Xe (λ≥420), CH_3OH	29375	17
LSPCN10 (Present research)	150 W Xe (λ≥420), CH_3OH	32975	

References

1. J. Ni, J. Xue, L. F. Xie, J. Shen, G. He and H.Chen, Construction of magnetically separable NiAl LDH/Fe_3O_4-RGO nanocomposites with enhanced photocatalytic performance under visible light, *Phys. Chem. Chem. Phys*., 2018, **20**, 414-421.
2. J. Liang, Y. Wei, Y. Yao, X. Zheng, J. Shen, G. He and H. Chen, Constructing high-efficiency photocatalyst for degrading ciprofloxacin: Three-dimensional visible light driven graphene based NiAlFe LDH, *J Colloid Interf Sci*., 2019, **540***,* 237-246.
3. Z. Liu, J. Tian, C. Yu, Q. Fan, X. Liu, K. Yang, J. Zeng and H. Ji, Ultrasonic fabrication of SO_4^{2-} doped g-C_3N_4/Ag_3PO_4 composite applied for effective removal of dyestuffs and antibiotics, *Mater. Chem. Phys*., 2020, **240***,* 122206.
4. Y. Deng, L. Tang, C. Feng, G. Zeng, J. Wang, Y. Zhou, Y. Liu, B. Peng and H. Feng, Construction of plasmonic Ag modified phosphorous-doped ultrathin g-C_3N_4 nanosheets/$BiVO_4$ photocatalyst with enhanced visible-near-infrared response ability for ciprofloxacin degradation, *J. Hazard. Mater*., 2018, **344,** 758-769.
5. H. Zhang, , W. Wu, Y. Li, Y. Wang, C. Zhang, W. Zhang, L. Wang, and L. Niu, Enhanced photocatalytic degradation of ciprofloxacin using novel C-dot@ Nitrogen deficient g-C_3N_4: synergistic effect of nitrogen defects and C-dots. *Appl. Surf. Sci.,* 2019, **465**, 450-458.
6. Z. Yang, , J. Yan, J. Lian, H. Xu, X. She and H. Li, g-C_3N_4/TiO_2 Nanocomposites for Degradation of Ciprofloxacin under Visible Light Irradiation, *Chemistry Select,* 2016, **1**, 5679-5685.
7. V. Jayaraman and A. Mani, Ag, Ni bimetallic supported g-C_3N_4 2D/$Cd_2Sb_2O_{6.8}$ pyrochlore interface photocatalyst for efficient removal of organic pollutants, *J. Mater. Sci-Mater. El.,* 2020, **31**, 11247-11267.
8. G. Zhang, B. Lin, Y. Qiu, L. He, Y. Chen and B. Gao, Highly efficient visible-light-driven photocatalytic hydrogen generation by immobilizing CdSe nanocrystals on ZnCr-layered double hydroxide nanosheets, *Int. J. Hydrogen Energ.*, 2015, **40,** 4758-4765.
9. L. Yao, D. Wei, D. Yan and C.Hu, ZnCr Layered Double Hydroxide (LDH) Nanosheets Assisted Formation of Hierarchical Flower-Like CdZnS@LDH Microstructures with Improved Visible-Light-Driven H_2 Production, *Chem. Asian J.,* 2015, **10,** 630−636.
10. S. Nayak, L. Mohapatra and K. M. Parida, Visible light-driven novel g-C_3N_4/NiFe-LDH composite photocatalyst with enhanced photocatalytic activity towards water oxidation and reduction reaction*, J. Mater. Chem. A,* 2015, **3,** 18622-18635.

11. R. Boppella, C. H. Choi, J. Moon and D. H. Kim, Spatial charge separation on strongly coupled 2D-hybrid of rGO/$La_2Ti_2O_7$/NiFe-LDH heterostructures for highly efficient noble metal free photocatalytic hydrogen generation, *Appl. Catal., B: Environ*., 2018, **239***,* 178−186.
12. J. M. Lee, J-H.Yang, N. H. Kwon, Y. K. Jo, J-H. Choy and S-J. Hwang, Intercalative Hybridization of Layered Double Hydroxide Nanocrystal with Mesoporous g-C_3N_4 for Enhancing Visible Light-Induced H_2 Production Efficiency, *Dalton Trans.,* 2018, **47**, 2949-2955.
13. L. Liu, X. Xu, Z. Si, Z. Wang and R. Ran, Y. He and D.Weng, Noble metal-free NiS/P-S codoped g-C_3N_4 photocatalysts with strong visible light absorbance and enhanced H_2 evolution activity, *Catal. Commun*., 2018, **106,** 55-59.
14. T. Su, Z. D. Hood, M. Naguib, L. Bai, S. Luo, C. M. Rouleau, I. N. Ivanov, H. Ji, Z. Qin and Z. Wu, 2D/2D heterojunction of Ti_3C_2/g-C_3N_4 nanosheets for enhanced photocatalytic hydrogen evolution, *Nanoscale,* 2019, **11**, 8138-8149.
15. J. Zhang, Q. Zhu, L. Wang, M. Nasir, S. –H. Cho and J. Zhang, g-C_3N_4/CoAl-LDH 2D/2D hybrid heterojunction for boosting photocatalytic hydrogen evolution, *Int. J. Hydrogen Energ.,* 2020.
16. D. P. Sahoo, S. Nayak, K. H. Reddy, S. Martha and K. Parida**,** Fabrication of a $Co(OH)_2$/ZnCr LDH "p–n" heterojunction photocatalyst with enhanced separation of charge carriers for efficient visible-light-driven H_2 and O_2 evolution, *Inorg. chem*., 2018, **57,** 3840-3854.
17. D. P. Sahoo, S. Patnaik and K. Parida, Construction of a Z-Scheme Dictated WO_{3-X}/Ag/ZnCr LDH Synergistically Visible Light-Induced Photocatalyst towards Tetracycline Degradation and H_2 Evolution. *ACS Omega*, 2019, **4,** 14721-14741.